

16.4 SENSITIVITY OF TORNADOGENESIS IN VERY-HIGH RESOLUTION NUMERICAL SIMULATIONS TO VARIATIONS IN MODEL MICROPHYSICAL PARAMETERS

Nathan A. Snook* and Ming Xue
University of Oklahoma, Norman, Oklahoma

1. INTRODUCTION

With the recent improvement in numerical weather prediction (NWP) models and data assimilation techniques, together with the rapid increase in computational power, explicit predictions of both organized convective systems and individual convective storms have become a reality. As data assimilation techniques improve, the errors or uncertainties in the prediction model start to become a major issue. In fact, model errors affect both prediction and data assimilation. For short-range convective-scale data assimilation and prediction, the model microphysics scheme appears to be the largest source of uncertainty hence potential error. Most commonly used microphysics schemes employ the 'bulk' approach of parameterization, in which the particle or drop size distributions (DSD's) are parameterized in functional forms. Often, significant uncertainties exist with the treatment of microphysical processes and microphysical parameters. Previous sensitivity studies (e.g. Gilmore et

al. 2004; Tong and Xue 2006) demonstrate that the structure and evolution of simulated convective systems are very sensitive to microphysical parameterizations. Variations in microphysical parameters, such as collection efficiencies, DSD parameters and particle densities, have profound effects upon the characteristics of precipitation systems and their associated dynamical processes.

In this study, we perform a set of idealized numerical simulations of supercell storms, using a horizontal resolution of 100 m, sufficient to explicitly simulate the genesis and life cycle of tornado(s) within the supercell. We vary the DSD-related parameters within an ice microphysics scheme employed by the simulation model to examine the sensitivity of tornadogenesis to these microphysical parameters. Through an analysis of the simulations, physical explanations as to the reasons for such sensitivities are offered.

Table 1. Summary of experiments, and the resolutions at which they are run.

Experiment name	Intercept parameter			Hail density (kgm ⁻³)	Characteristics	Resolution
	Rain	Hail	Snow			
CNTL	8×10^6	4×10^4	8×10^6	900	Control	1 km/100 m
H2	8×10^6	4×10^2	8×10^6	900	Large hailstones	1 km/100 m
H6	8×10^6	4×10^6	8×10^6	900	Small hailstones	1 km/100 m
R5	8×10^5	4×10^4	8×10^6	900	Large raindrops	1 km/100 m
R7	8×10^6	4×10^4	8×10^6	900	Small raindrops	1 km/100 m
H2R5	8×10^5	4×10^2	8×10^6	900	Large hailstones and Raindrops	1 km/100 m
H6R7	8×10^7	4×10^6	8×10^6	900	Small hailstones and Raindrops	1 km/100 m
Kessler	8×10^6	N/A	N/A	N/A	Kessler warm rain microphysics	1 km
S7	8×10^6	4×10^4	8×10^7	900	Small snowflakes	1 km
S8	8×10^6	4×10^4	8×10^8	900	Very small snowflakes	1 km
D400	8×10^6	4×10^4	8×10^6	400	Low hail density	1 km
H2D400	8×10^6	4×10^2	8×10^6	400	Low hail density, Large raindrops	1 km
R5D400	8×10^5	4×10^4	8×10^6	400	Low hail density, Large hailstones	1 km

2. EXPERIMENT DESIGN

The Advanced Regional Prediction System (ARPS), Version 5, is used to perform the numerical simulations in this study. The ARPS is a compressible, non-hydrostatic NWP model suitable for storm-scale simulation and prediction. The most used microphysics option in ARPS-based studies is a scheme based on Lin

*Corresponding author address: Nathan A. Snook, School of Meteorology, University of Oklahoma, 120 David L. Boren Blvd. Suite 5900, Norman, OK, 73072; e-mail: nsnook@ou.edu

et al. (1983, LFO83 hereafter). The LFO83 scheme is also the basis for a number of other commonly used schemes (e.g., Gilmore et al. 2004; Hong and Lim 2006). The scheme calculates the mixing ratios of six water species; water vapor, cloud water, cloud ice, rain, snow, and hail; it deals with the complex processes of

the production of and conversions among these different species. It assumes an inverse-exponential DSD consistent with Marshall and Palmer (1948) for rain, snow, and hail, and a monodisperse DSD for cloud water and cloud ice.

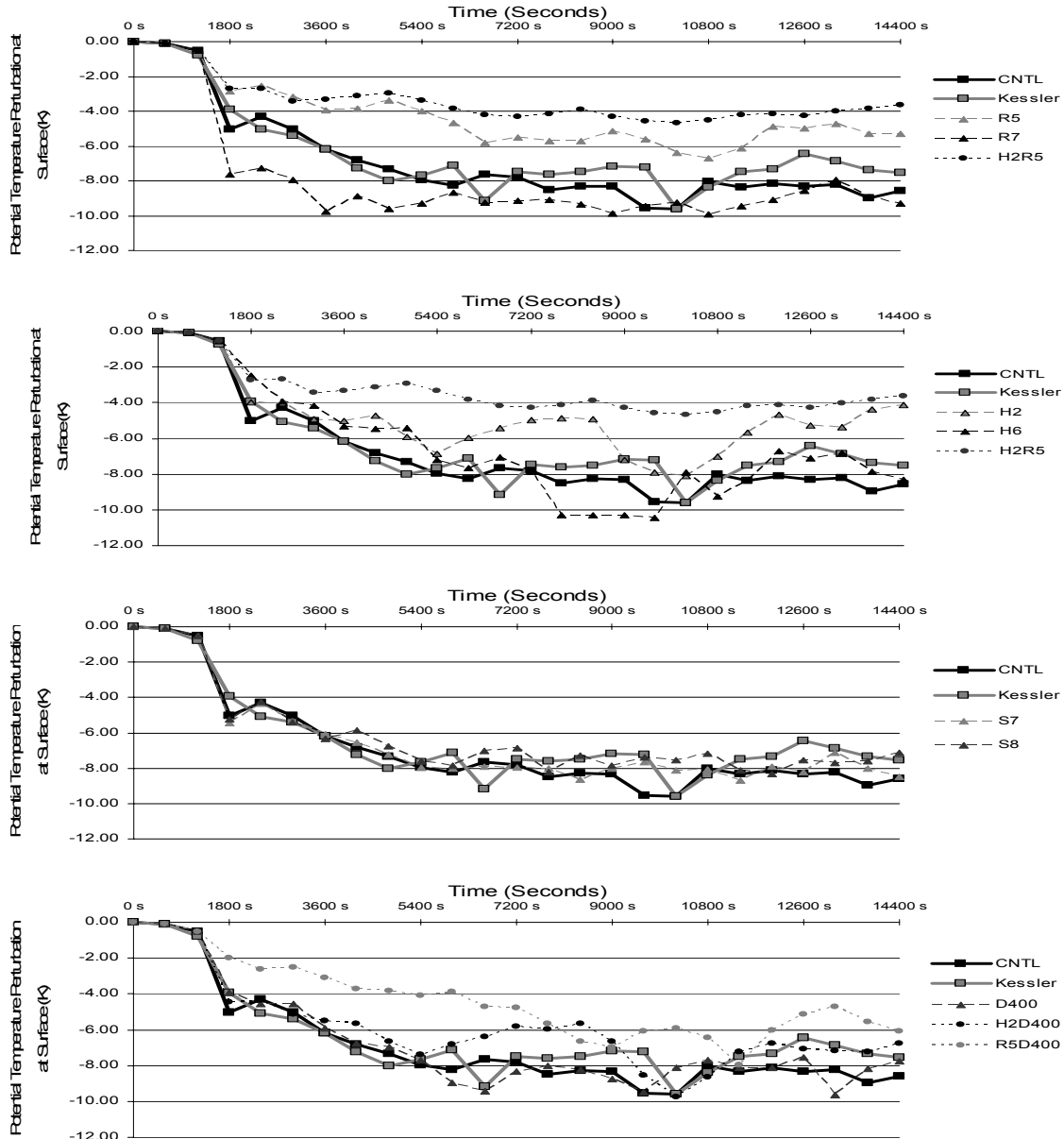


Fig. 1. Timeseries of surface cold pool intensity for low-resolution (1 km horizontal grid spacing) simulations varying (a) hail intercept parameter, (b) rain intercept parameter, (c) snow intercept parameter, and (d) hail density. Dotted lines show simulations containing variations in two parameters. CNTL and Kessler runs are provided in each plot for comparison.

Two sets of simulations were conducted; they include thirteen 1 km horizontal-resolution simulations (the low-resolution set) and seven 100 m horizontal-resolution simulations (the high-resolution set). Details concerning the configuration for each of the simulations can be found in Table 1. In each of the simulations, one

or more intercept parameters were varied for rain, snow, or hail, along with possible variation in hail density. Control values were based on default settings in LFO83, and the increased and decreased values used in experiments were chosen to fall within the range

observed values of previous studies (Waldvogel 1974), (Lo, 1982).

For the low-resolution simulations a larger physical domain of $128 \times 128 \times 16 \text{ km}^3$ is used, with 35 vertical levels and the vertical grid spacing increasing from 100 m near the surface to 700 m near the model top. For the high-resolution simulations, a smaller domain of $64 \times 64 \times 16 \text{ km}^3$ is used, with 81 vertical levels and the vertical grid spacing increasing from 10 m to 700 m.

3. RESULTS AND DISCUSSION

The goal of the 1 km low-resolution simulations was to determine which microphysical parameters were most influential on supercell dynamics and on tornado potential. In Fig. 1 is a plot of the maximum cold pool intensity, in terms of the minimum potential temperature perturbation (θ') at the first grid level above surface within the domain, for selected 1 km runs. Cold pool intensity is selected as an indicator of low-level dynamical sensitivity because it has a strong effect on storm propagation and on the baroclinic generation of low-level horizontal vorticity, which in turn influences tornado potential (Rotunno and Klemp 1985). The cold pool intensity also has a strong effect on the updraft intensity and orientation in convective systems (Rotunno et al. 1988). Fig. 1 shows a great deal of variation in the cold pool intensity among different simulations. The greatest departure from the control run (CNTL) was obtained by altering the rain intercept parameter. Varying the hail intercept parameter yielded slightly less departure, and variations in the snow intercept parameter and hail density yielded very little departure from CNTL. The results of the low-resolution simulations, along with those of all other simulations conducted in this study, will be discussed in greater detail in a future manuscript (Snook and Xue, to be submitted).

The 1 km simulations show that the rain and hail intercept parameters have the largest influence on the cold pool intensity and the storm dynamics in general. We

therefore focus exclusively in the high-resolution simulations on the effects of these two parameters. Seven 100-m horizontal-resolution experiments are conducted, varying the rain and hail intercept parameters (Table 1). They include the control simulation (CNTL), two simulations varying the rain intercept parameter (R5 and R7), two simulations varying the hail intercept parameter (H2 and H6), and two simulations varying both rain and hail intercept parameters (H2R5 and H6R7).

Simulations DSDs favoring larger hydrometeors (H2, R5, and H2R5) correspond to the weakest cold pools. Combining larger raindrops and larger hailstones seem to have an additive effect, with H2R5 exhibiting the weakest cold pool of all. The opposite is true for simulations with DSDs favoring smaller hydrometeors (H6, R7, and H6R7); in these simulations the cold pool is more intense than in CNTL and experiments favoring larger hydrometeors than CNTL. One cause of these results is the differences in evaporative cooling among different simulations, which result from two major sources: variation in areal coverage and intensity of precipitation, and changes in total droplet surface area. In those simulations with DSDs favoring larger rain drops, for the same total volume of rain water, the total surface area for rain drops is smaller therefore the rain evaporation is less as the rain drops fall. As a result, more evaporation can take place when the DSD favors small raindrops, enhancing the evaporative cooling that results. Similar is true for hailstones. In addition, smaller droplets are lighter and have a lower terminal velocity; they are more readily advected further away from the main updraft and fall out over a wider area. The result is a larger geographic distribution of evaporative cooling, and thus a cold pool with more areal coverage. These conclusions are supported by Fig. 2, which show that in H2R5 areas of light rain are diminished but the cores of intense rainfall exist because the larger, heavier raindrops with their larger terminal velocities are not advected far downwind before falling to the surface.

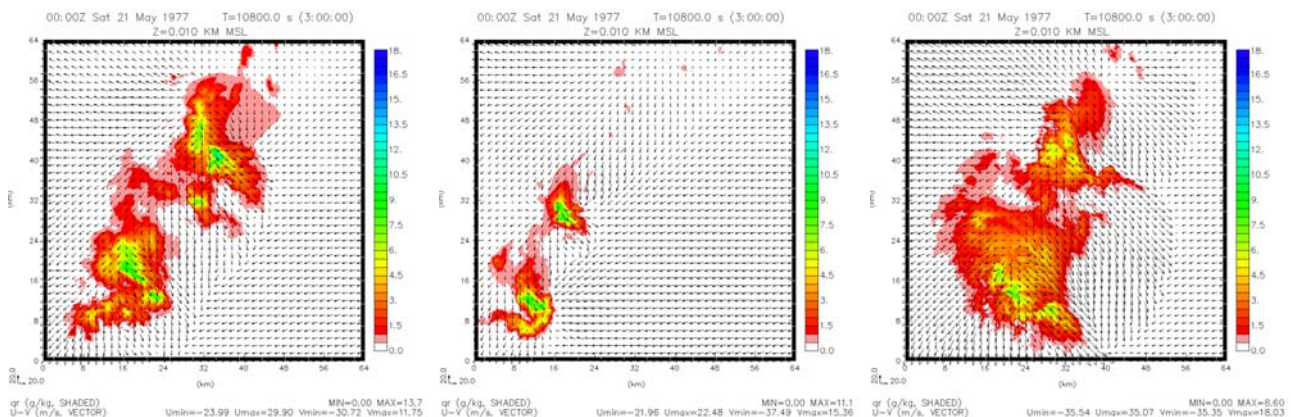


Fig. 2. Plot of rainwater mixing ratio (color-fill) and horizontal wind fields (vectors), 10 m above the surface at 3 hours of model time. Shown are CNTL (left), H2R5 (center), and H6R7 (right).

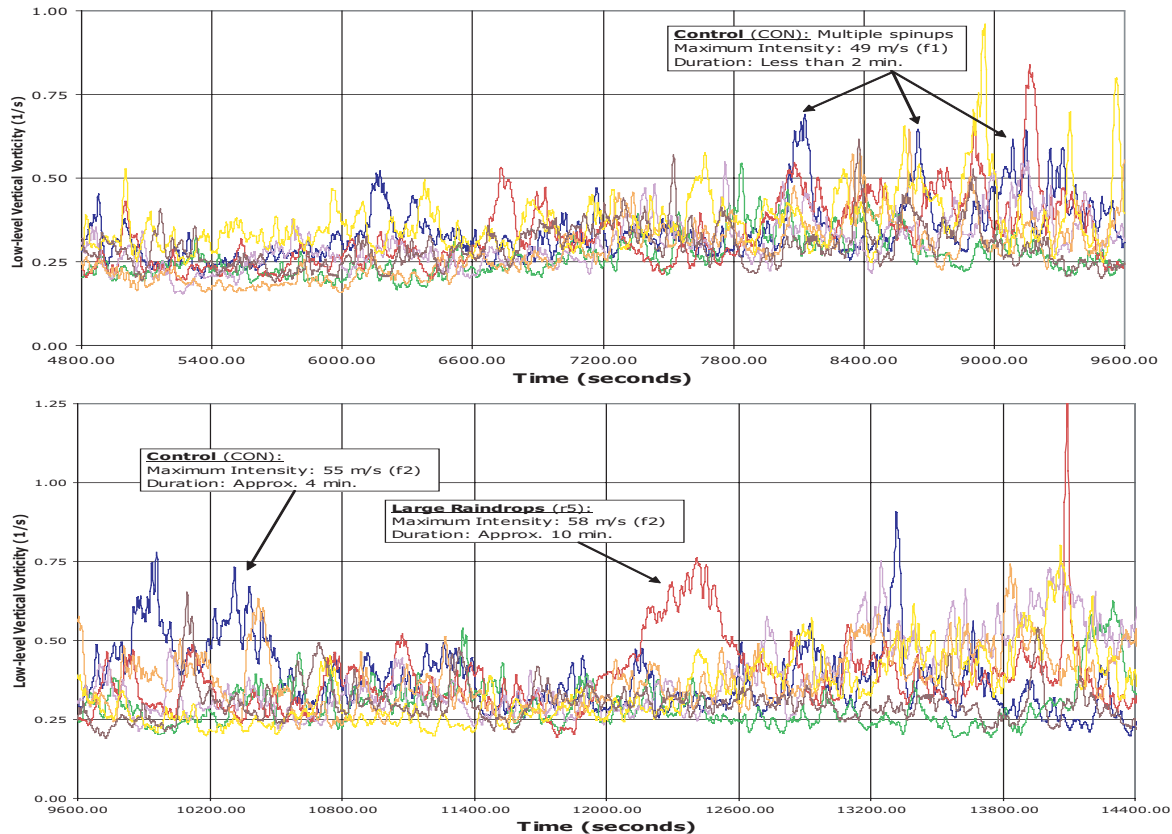


Fig. 3. Time series of maximum low-level (below 2 km) cyclonic vertical vorticity for the seven 100 m resolution simulations. Prominent tornadic circulations are noted, along with duration and Fujita scale intensity, for 4800 s to 9600 s, and 9600 s to 14000 s of model time.

By contrast, variation in the hail intercept parameter has only a weak direct effect on evaporative cooling, but a stronger influence on the distribution and intensity of rainfall (not shown).

Strong, long-lived tornadic surface vortices are observed in two of seven 100 m simulations: CNTL and R5, which are noted in Fig. 3. The surface vortex in CNTL lasts for approximately 4 minutes, with a maximum low-level wind speed of 55 m s^{-1} , which gives the tornado an F2 intensity on the Fujita scale. The surface vortex in R5 lasts approximately 10 minutes, with a maximum surface wind speed of 58 m s^{-1} (also F2 intensity). These tornadoes occur in CNTL and R5 which have well-defined supercells and weak to moderate cold pool intensity. In contrast, all surface vortices that form in simulations with the strong cold pool are weak and very short lived.

In control experiment CNTL, two tornadic events occur: between 8400 and 9600 s, a series of very brief, short-lived tornadic spin-ups take place. These spinups are located beneath the mid-level mesocyclone, near the interface of the storm's rear flank and forward flank gust fronts. At the time of tornadogenesis, the forward flank gust front is present, but somewhat diffused and poorly defined. These events are all very brief, lasting no more than two minutes, and the maximum wind speed in these spin-ups never exceeds 50 m s^{-1} , putting these short-lived tornadoes within the F0 to F1 range on

the Fujita scale. A more long-lived tornadic vortex of F2 intensity is present between 12300 and 12600 s, lasting between 4 and 5 minutes, and achieving a maximum wind speed of approximately 55 m s^{-1} . In experiment R5, which favors larger raindrops, a single intense tornado is present approximately between 12,000 s and 12,720 s, lasting for about 10 minutes and attaining a maximum wind speed of 58 m s^{-1} (F2). Like the control run, two supercell thunderstorms are present within the model domain, and all tornadic activity is associated with the northern storm. The tornadic circulation begins to develop near the tip of the hook echo, beneath the mid-level mesocyclone, and at the interface of the rear flank and forward flank gust fronts. Unlike in CNTL, the forward flank gust front in R5 is much better defined. The tornado reaches its maximum intensity about five minutes later at 12,360 s, and attains a diameter of approximately 700 m, or 7 times the minimum grid resolution. The tornado persists at near maximum intensity for about 2 minutes, until around 12,480 s, and then begins a steady weakening trend until its end around 12,720 s. A plot of the reflectivity, vorticity, and surface wind for this tornado, near its peak intensity, are shown in Fig. 4. The tornadic circulation, embedded within the hook echo of its parent supercell is clearly visible. Because the tornado in R5 is located beneath its parent mesocyclone, it probably benefits more from the dynamical forcing than that in CNTL.

Fig. 5 shows the trajectories of the air parcels originating from the low-level inflow region ahead of the forward flank gust front, in R5 and H6R7. Parcels were released into the inflow at such time that they would enter a mature cell near its peak intensity. In R5, the inflow parcels begin near the surface, and are drawn southwest relative to the storm, remaining near the surface until entering the updraft and rising with a moderate westward slope to the mid-levels, followed by a nearly vertical ascent to the upper levels of the storm. Some of the parcels reach altitudes of nearly 14 km before sinking, indicating a storm with vigorous updraft and an overshooting top. While ascending from near the surface to mid levels (4 km altitude) the parcels moved an average of 2 km horizontally, for a resulting steep updraft slope of 2 over 1. The parcels within the inflow region of the storm in H6R7 similarly began by moving southwestwards near the surface, but upon entering the updraft they maintained a strong westward component in their trajectory as they rose to the mid-levels, with somewhat more vertical motion when entering the upper part of the updraft. The parcels in the inflow of H6R7 move an average of 6 km horizontally while they rise from near the surface to the mid-levels (4 km altitude), giving an updraft slope of 0.67. The results of this trajectory analysis further highlight the difference in the updraft structure.

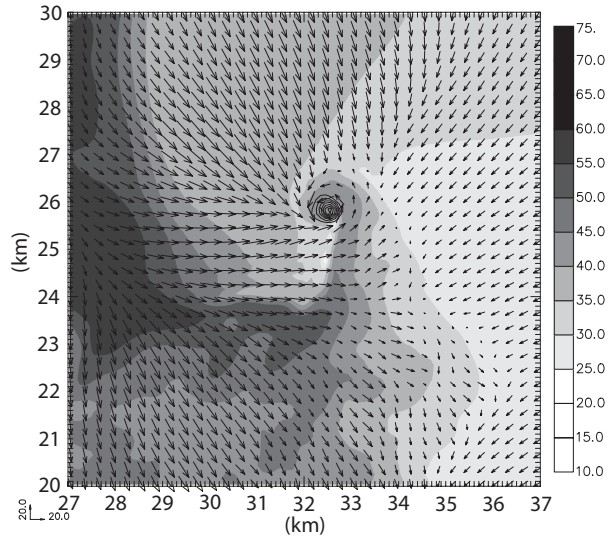


Fig. 4. Zoomed-in view of the tornadic circulation in R5. Tornado is shown near its maximum intensity. Plotted are radar reflectivity (dBZ, grayscale), vertical vorticity (contour), and wind vectors 10 m above the surface.

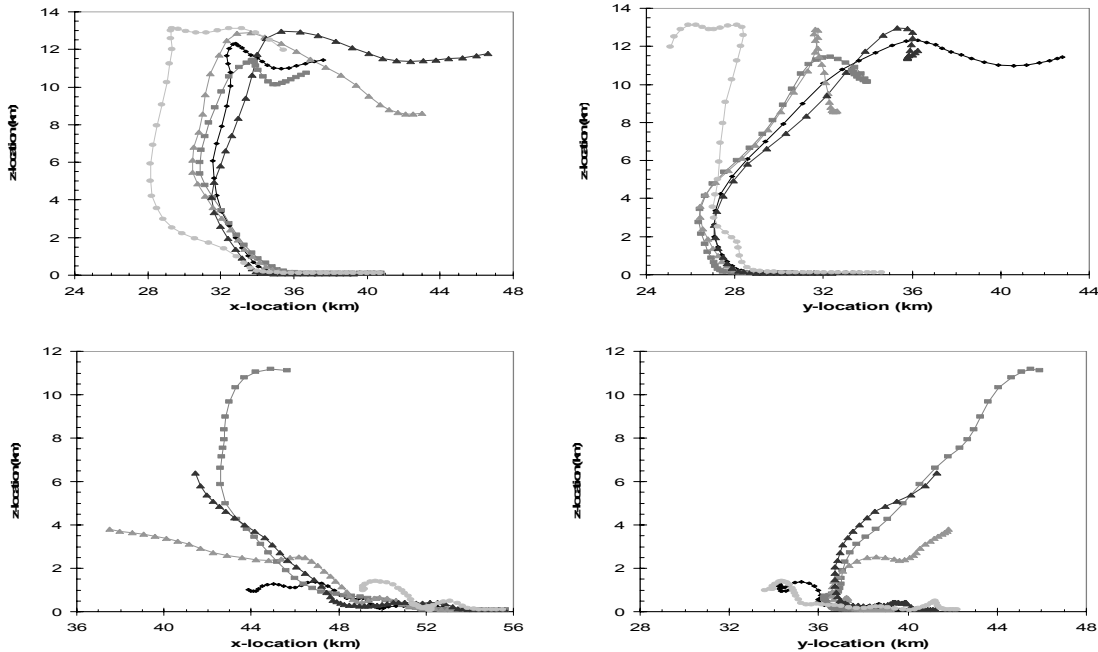


Fig. 5. Time-dependent trajectories in the x-z (left panels) and y-z (right panels) planes, of parcels initially located within the inflow region of the storms in R5 (a and b) and H6R7 (c and d). Planes along the trajectories are separated by 30 seconds, with trajectories calculated at times when mature, fully developed storm cells were present.

4. SUMMARY AND CONCLUSIONS

In this study we have demonstrated that numerical simulations of supercell thunderstorms are highly

sensitive to DSD parameters in a commonly-used single-moment ice microphysics scheme, both at horizontal resolutions of 1 km and 100 meter. Using the Lin et al. (1983) ice microphysics scheme and varying only the intercept parameter for the Marshall-Palmer-like

inverse-exponential DSD's of rain and hail, we obtained widely varying model solutions, including single and multiple supercells and a linear system, from the same set of initial and environmental conditions. We have shown that cold pool intensity and geographical coverage, precipitation intensity and amount, updraft speed and orientation, and tornado potential all show significant sensitivity to variations in rain and hail intercept parameters. The sensitivities to microphysical parameters observed in this study are generally consistent with the findings of Adlerman and Droegemeier (2002), Gilmore et al. (2004), and van den Heever and Cotton (2005), whose simulations are limited to the 1 km horizontal resolution and the exploration of few microphysical parameters.

Simulations at the 1 km horizontal resolution reveal that, of the parameters tested, cold pool intensity and low-level supercell dynamics are most sensitive to variations in the rain and hail intercept parameters and much less sensitive to the snow intercept parameter and hail density. While rain and hail are present in high concentrations near the surface and at the mid-levels, snow in this case is present only in the upper levels and in the anvil region of the storm, lessening its impact on low-level dynamics and properties such as cold pool strength and potential for tornadogenesis.

When the DSD used favors large hydrometeors, the resulting simulations exhibit weak cold pool intensity. Reduced total hydrometeor surface area leads to less evaporation of hydrometeors passing through unsaturated air, reducing total evaporative cooling. In addition, the larger hydrometeors, with their greater terminal velocity, are not advected very far from the updraft before falling to the surface, reducing the geographical coverage of the precipitation core, further limiting the cold pool intensity. This weak cold pool, induced by reduced evaporative cooling, produces supercell storms with steady, strong updrafts, and high tornado potential due to a favorable gust front that allows for vertically oriented updrafts and better alignment of low-level and mid-level vorticity centers. By contrast, when the DSD favors smaller hydrometeors, the resulting simulations contain many smaller hydrometeors, with a much greater total surface area for evaporation, and a low terminal velocity. Thus the storms produced exhibit intense cold pools due to enhanced evaporative cooling over a larger geographical area, producing cyclic supercells or linear convective systems. These storms tend to have weak, pulsing updrafts that slant rearward with height and low tornado potential, due in part to strong gust fronts that often outrun their parent storms by several kilometers.

Finally, we note that while we believe the conclusions drawn in this paper about the very large sensitivity of thunderstorm dynamics and tornado potential to microphysical parameters and the mechanism of sensitivity are robust, tornadoes do not necessarily form when the cold is colder or warmer. There is probably a balance between the cold pool strength and environmental flow, and the storm dynamics will certainly also be influenced by other parameters of the storm environment, including

convective available potential energy (CAPE). Intense supercell tornadoes would only occur when many conditions are favorable, including the presence of an intense rotating updraft located almost directly over the low-level center of rotation. Full understanding of tornadogenesis will require much more research.

Acknowledgement: This work was primarily supported by NSF grant EEC-0313747. Ming Xue was further supported by NSF grants ATM-0530814, ATM-0331594 and ATM-0331756.

5. REFERENCES

- Adlerman, E. J. and K. K. Droegemeier, 2002: The Sensitivity of Numerically Simulated Cyclic Mesocyclogenesis to Variations in Model Physical and Computational Parameters. *Mon. Wea. Rev.*, **130**, 2671-2691.
- Gilmore, M. S., J. M. Straka, and E. N. Rasmussen, 2004: Precipitation uncertainty due to variations in precipitation particle parameters within a simple microphysics scheme. *Mon. Wea. Rev.*, **132**, 2610-2627.
- Hong, S.-y. and J.-O. J. Lim, 2006: The WRF single-moment 6-class microphysics scheme (WSM6). *J. Korean Meteor. Soc.*, **42**, 129-151.
- Lin, Y.-L., R. D. Farley, and H. D. Orville, 1983: Bulk parameterization of the snow field in a cloud model. *J. Climate Appl. Meteor.*, **22**, 1065-1092.
- Lo, K. K. and R. E. Passarelli Jr., 1982: The Growth of Snow in Winter Storms: An Airborne Observational Study. *J. Atmos. Sci.*, **39**, 697-706.
- Marshall, J. S. and W. M. Palmer, 1948: The distribution of raindrops with size. *J. Meteor.*, **5**, 165-166.
- Rotunno, R. and J. B. Klemp, 1985: On the rotation and propagation of simulated supercell thunderstorms. *J. Atmos. Sci.*, **42**, 271-292.
- Snook, N. and M. Xue, 2007: Sensitivity of Tornadic Thunderstorms and Tornadogenesis in Very-high Resolution Numerical Simulations to Variations in Model Microphysical Parameters. *J. Atmos. Sci.*, To be submitted.
- Tong, M. and M. Xue, 2006: Simultaneous estimation of microphysical parameters and atmospheric state with radar data and ensemble square-root Kalman filter. Part I: Sensitivity analysis and parameter identifiability *J. Atmos. Sci.*, Submitted.
- van den Heever, S. C. and W. R. Cotton, 2004: The Impact of Hail Size on Simulated Supercell Storms. *J. Atmos. Sci.*, **61**, 1596-1609.
- Waldvogel, A., 1974: The N0-jump of raindrop spectra. *J. Atmos. Sci.*, **31**, 1067-1078.